JOURNAL OF PROPULSION AND POWER
Vol. 14, No. 3, May–June 1998

Sound-Pressure-Level Variations in a Supersonic Rectangular Cavity at Yaw

Peter J. Disimile* and Paul D. Orkwis†
University of Cincinnati, Cincinnati, Ohio 45221-0070

An experimental investigation was undertaken to examine the effect of yaw angles on flow oscillations that occur within an open cavity at $M_\infty = 2$. A rectangular cavity with a length-to-depth ratio of 2 and a planar aspect ratio of 11.83 was placed within a thick turbulent boundary layer with a corresponding $Re_\theta = 7.3 \times 10^4$. Pressure–time histories were acquired at 25 separate yaw angles using high-speed pressure transducers. These signals were analyzed and the sound pressure levels and dominant frequencies determined. This study indicates that large changes in the sound pressure level occur as the yaw angle is changed from 0 to 70 deg. Further, evidence suggesting a mode switch from a transverse acoustic mode at yaw angles less than approximately 40 deg to a fluid dynamic mode for yaw angles >45 deg is presented.

Nomenclature

a_T = speed of sound within the cavity based on the stagnation temperature, m/s
c_f = local coefficient of skin friction
D = cavity depth, the dimension between the cavity floor and top surface, cm
f_D = fundamental acoustic mode based on cavity depth, Hz
f_L = fundamental acoustic mode based on cavity length, Hz
f_V = vortex shedding frequency, Hz
f_W = fundamental acoustic mode based on cavity width, Hz
$f_{e,m}$ = Rossiters edge-tone frequency for mode m, Hz
H = boundary-layer shape factor
L = cavity dimension along the minor axis, cm
L/D = cavity length-to-depth ratio
M_∞ = freestream Mach number
m = acoustic mode number, i.e., 1, 2, 3, . . . , used in Rossiters equation
p = surface pressure, kPa
$\bar{p}$ = time-averaged surface pressure, kPa
$\overline{p'^2}$ = mean-squared fluctuating pressure, kPa^2
q_a = acoustics reference level, 20×10^{-6}, Pa
Re_θ = Reynolds number based on the boundary-layer momentum thickness
$\overline{\text{SPL}}$ = sound pressure level, dB
St_θ = Strouhal number based on the boundary-layer momentum thickness, $f_v\theta/U_\infty$
U = local mean velocity, m/s
U_∞ = freestream velocity, m/s
W = cavity dimension along the major axis, cm
W/L = cavity width-to-length ratio
δ^* = displacement thickness of the approaching boundary layer at location A, mm
θ = momentum thickness of the approaching boundary layer at location A, mm
ψ = yaw, the angle between U_∞ and cavity minor axis L, deg

Received April 19, 1997; revision received Dec. 19, 1997; accepted for publication Dec. 22, 1997.

*Associate Professor, Aerospace Engineering and Engineering Mechanics. Member AIAA.
†Assistant Professor, Aerospace Engineering and Engineering Mechanics. Senior Member AIAA.

Introduction

THE presence of a cavity in a surface bounding a fluid flow can cause large pressure, velocity, and density fluctuations in its vicinity, as well as strong propagating acoustic waves. Although these fluctuations are usually unwanted and are typically addressed as an external aerodynamics problem, similar concerns also exist for internal flows. For example, such oscillations can cause sensitive instrumentation within a propulsion system to be damaged or can calibrations biased, can result in the generation of noise, or can cause structural vibration and fatigue because of resonance. However, there are situations where these flow oscillations can be used to improve a given process, such as to provide enhanced mixing and heat transfer, or used as a flow-rate indicator. Oscillations in internal flows are of interest in many different areas of engineering, from scramjet combustors to gasdynamic lasers.

Supersonic cavity flowfields contain a mixture of unsteady flow regimes that may include unstable shear layers that shed vortices in coherent patterns, unsteady weak shock or pressure waves, and resident vortices oriented in the transverse direction. The shear-layer location and generation of self-sustaining oscillations depend upon conditions both inside and outside the cavity, and in turn influence the internal and external flow fields about the cavity. This interaction is the result of an extremely complicated flow pattern that appears to depend upon the shape of the cavity, Mach number, Reynolds number, and characteristics of the approaching boundary layer.[1] Based on the work of Wilcox,[2] and Stallings and Forrest,[3] four types of mean cavity flow exist. These were summarized by Tracy and Plentovich[4] and are briefly listed in Table 1 for completeness (see Fig. 1). Self-sustaining oscillations found in cavity flows have also been grouped by Rockwell and Naudascher[5] as follows:

1) Fluid dynamic—oscillations arising from the combined effect of shear-layer instability amplification and feedback of downstream disturbances. The presence of large-scale vortical motions in the shear layer are believed to play a major role in this interaction. Standing acoustic waves are not involved in this mechanism, nor is compressibility or high M_∞ required.

2) Fluid resonant—oscillations influenced by standing acoustic waves within the cavity.

3) Fluid elastic—when motions of a solid boundary are coupled to the flow oscillations caused by nonlinear interactions between vortex shedding and acoustic wave phenomena.[6]

Table 1 Cavity classifications at supersonic speeds

Flow type	L/D	Comments
Closed (Fig. 1b)	≥ 13	The separating shear layer attaches to the cavity floor and again separates upstream of the aft cavity wall. The presence of acoustic tones has not been reported in this configuration.
Open (Fig. 1a)	≤ 10	A free shear layer is formed over the mouth of the cavity. Weak shock waves are found around the separation and reattachment points. High-intensity acoustic tones can develop.
Transitional (closed) (Fig. 1c)	$10 \leq L/D \leq 13$	Shock waves resulting from the shear-layer attachment and separation positions on the cavity floor coincide and become a single shock wave.
Transitional (open) (Fig. 1d)	$10 \leq L/D \leq 13$	The shear layer no longer attaches to the floor of the cavity. This condition can occur after a slight change in the L/D, when a transitionally closed flow exists.

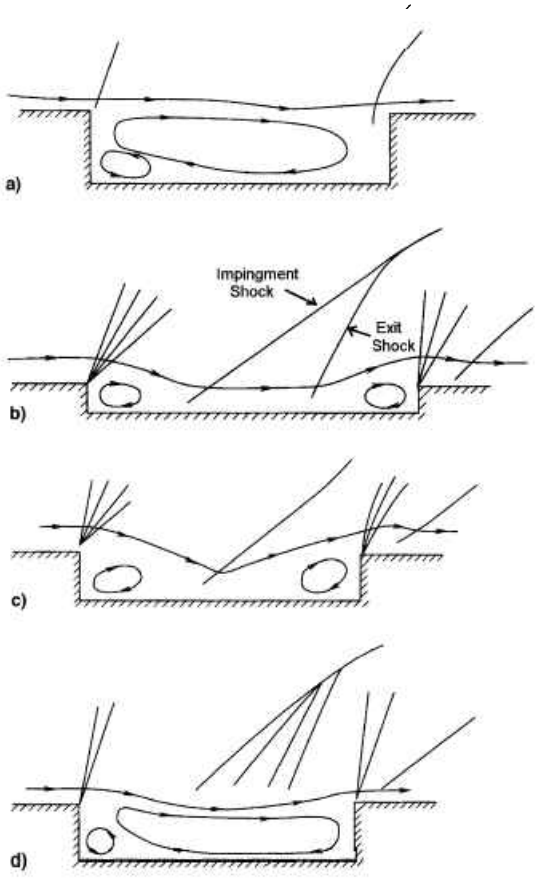

Fig. 1 a) Open, b) closed, c) transitionally closed, and d) transitionally open cavity flows.

Many prior investigations[7–10] have been conducted to gain insight into the underlying physical behavior of cavity flows. While none of these studies have been able to produce a universal understanding of the phenomena, empirical techniques including those of Rossiter[11] have made it possible to predict some features of the observed phenomena. Unfortunately, these investigations are limited to situations where the cavity width W spans the flow, i.e., the cavity is oriented at 0-deg yaw. Although limited information is available for yaw angles other than 0 deg,[5,12–16] all studies except for Bari and Chambers[15] and Savory et al.[16] examined a single second angle, either 15 or 45 deg. Bari and Chambers examined ψ from 0 to 30 deg; however, their flow was subsonic with a laminar boundary layer. Savory et al. only evaluated the mean drag for ψ between 0 and 90 deg; however, their subsonic boundary layer was turbulent. The goal of the present work is to systematically examine the effect of yaw on flow oscillations within an open cavity submerged in a supersonic turbulent boundary layer.

To accomplish this task an experimental program was undertaken using a single two-dimensional cavity model. A cavity was fabricated with a streamwise L/D of 2. The configured model, when orientated at 0-deg yaw, represented an open cavity, based on the classifications presented in Table 1. Results were obtained at yaw using a nominal W/L of 12, placed within a turbulent boundary layer at $M_\infty = 2$. The following sections provide details on the cavity model and facility as well as the results of this program.

Cavity Model

A rectangular cutout representing the cavity was configured from a segmented circular aluminum plug and placed within the wind tunnel (Fig. 2a). This plug had a diameter of 17.78 cm and could be rotated 180 deg. The rectangular opening in the cavity ($W \times L$) had dimensions of 12.38×1.05 cm, resulting in a planar aspect ratio W/L of 11.83. In the present tests the cavity floor was positioned 0.52 cm below the surface of the cavity, representing an L/D of 2. Figure 2b is a sketch of the cavity, designating the locations of high-speed pressure transducers.

Experimental Facility and Setup

The primary piece of hardware used in this research program was the University of Cincinnati's supersonic wind tunnel. This tunnel is configured as an intermittent blowdown facility, with a rectangular test section 15.24 cm wide by 16.54 cm high, extending downstream 45.7 cm. Tunnel operating conditions enable: $1.4 < M_\infty < 3.8$ and $27.6 <$ unit $Re < 82.7 \times 10^6$/m.

The cavity model was centrally located within the 16.54-cm test section sidewall. With the cavity oriented such that its width spanned the test section sidewall, approximately 2 cm remained between both sides of the cutout and the test section floor and ceiling. In this position W was aligned perpendicular to the oncoming boundary layer. This orientation is referred to as the 0-yaw case, where the effective streamwise length of the cavity was equal to the actual length L of the machined model.

Data-Acquisition Strategy

Thirty-four surface taps are located throughout the model for averaged surface pressure measurements. Pressure taps were placed 2.03 cm from either side of the centerline and 0.24 cm below the model surface to verify two dimensionality. To monitor flow oscillations in and around the cavity, three high-speed Entran EPI-080B miniature pressure transducers were mounted along the centerline of the model. A first transducer was positioned $0.25L$ upstream of the separation lip while a second was mounted on the cavity floor, $0.67L$ downstream from the base of the separation lip. The third and last high-speed transducer was located $0.31L$ past the aft lip of the cutout (Fig. 2b).

Transducer specifications provided by the manufacturer indicate a resonant frequency of 125 kHz and a flat response to more than 25 kHz. Based on comparison tests, the transducer

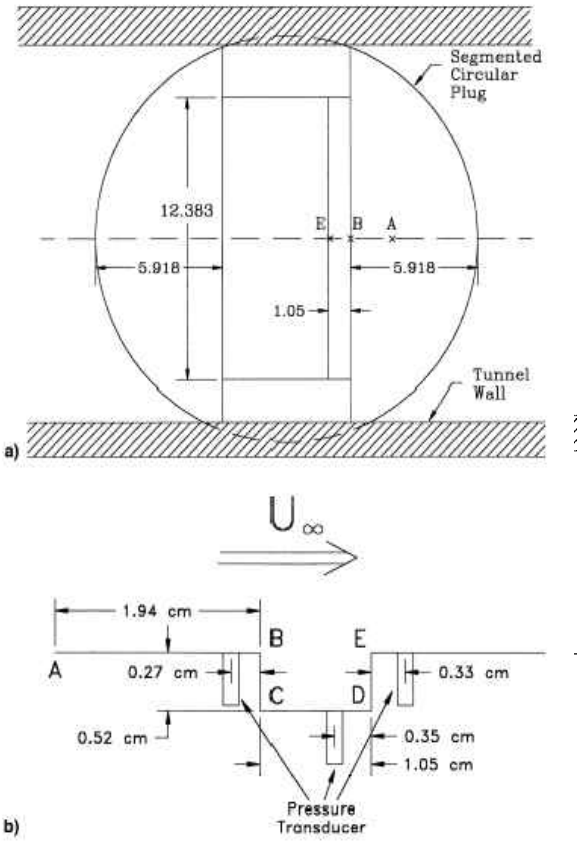

Fig. 2 Schematics of a) model within the test section and b) cavity model.

outputs were digitized at 50 kHz using an eight-channel, 16-bit simultaneous sample and hold A/D converter, and processed using a 486 microcomputer. This sampling rate was considered acceptable after acquisition of the pressure fluctuation levels in the upstream boundary layer were examined. During this process sampling rates of 50 and 100 kHz were tested. Because the results from the 50-kHz sampling frequency showed no discernible difference in the fast Fourier transform (FFT) content when compared to the 100-kHz case, the former sampling rate was selected.

Test Conditions

Test conditions for the present study were $M_\infty = 2$, and $Re_\theta = 7.3 \times 10^4$. The M_∞ profile and approaching wall boundary layer were documented prior to the acquisition of cavity data. A traversing total-pressure probe was employed to determine the total pressure profile across the test section. Both the boundary-layer and test-section traverses were acquired 1.94 cm upstream of the forward cavity wall. This location is designated as point *A*. Further, the probe was traversed across the test section at the centerline, as well as 2.54 and 5.08 cm above and below the centerline. A local M was calculated using the Raleigh–pitot formula. Figure 3 displays the M_∞ profiles obtained for the five planes. Each traverse was initiated at the sidewall that would eventually contain the model and extended across the test section to approximately 3.79 cm from the opposite wall. An averaged M_∞ within the test-section core was estimated as 1.98 ± 0.05.

Centerline total pressure traverses were repeated several times to verify repeatability and build a database. These data together with the total temperature and M_∞ calculated from the total pressure profiles were then used to estimate the local velocity. Based on the boundary-layer velocity profile the thickness of the boundary layer was estimated to be 13.9 mm. This supported the assumption that the test-section corner boundary layers were sufficiently far from the cavity sidewall. Therefore, it was assumed that the test-section corner flow would not dip into the cavity. A composite boundary-layer velocity profile resulting from four runs at the same centerline location is shown in Fig. 4. The worst-case velocity deviation throughout the boundary layer was 7%. Fitting a power-law profile to the measured velocity data resulted in a best-fit value of the exponent n of 8.4. In addition, these data provided an estimated c_f value of 0.0020. As a comparison, the Van Driest transformation was also performed on the centerline velocity profile, and a c_f value of 0.0021 was determined. Likewise, δ^*, θ, and H were calculated and determined to be nominally 2.8, 1.92, and 1.46 mm, respectively. Replotting the velocity distribution in wall coordinates, the data showed good agreement with the law of the wall between $250 < y^+ < 2{,}500$.

To complete the documentation of the test conditions the sound-pressure level and frequency content of the upstream boundary layer were recorded. Specifically, the pressure signals were acquired for two cases using the high-speed pressure transducer positioned upstream of the separation lip (Fig. 2). In the first case the cavity floor was positioned such that $L/D = 2$, and in the second case the cavity was eliminated. It was determined that the presence of the cavity produced no significant difference in the pressure signals received from the boundary-layer transducer. Therefore, regardless of the unsteadiness apparent in the cavity, no significant disturbances were communicated upstream along the wall through the

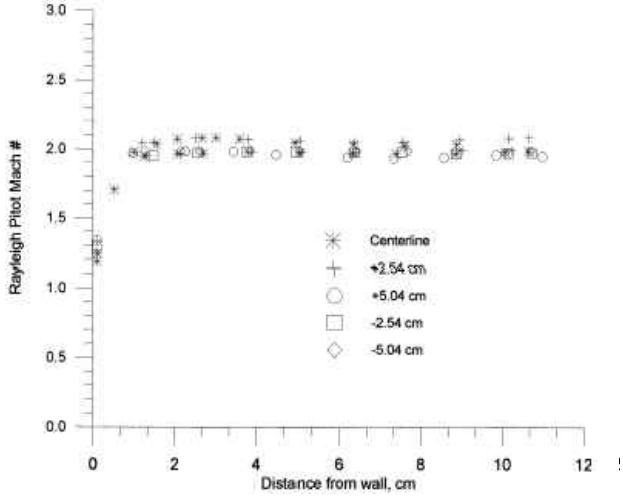

Fig. 3 Test section Mach number profile.

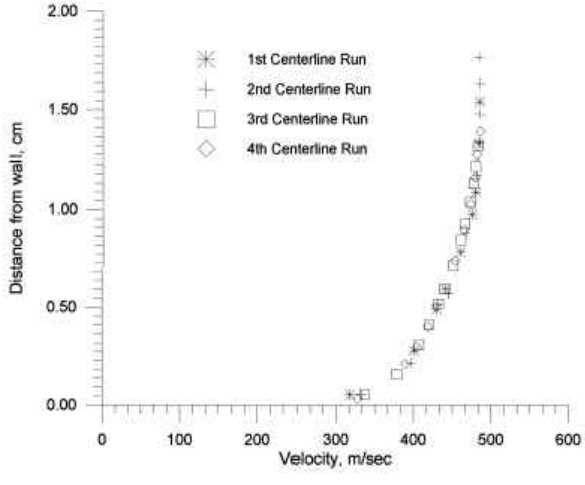

Fig. 4 Boundary-layer velocity distribution.

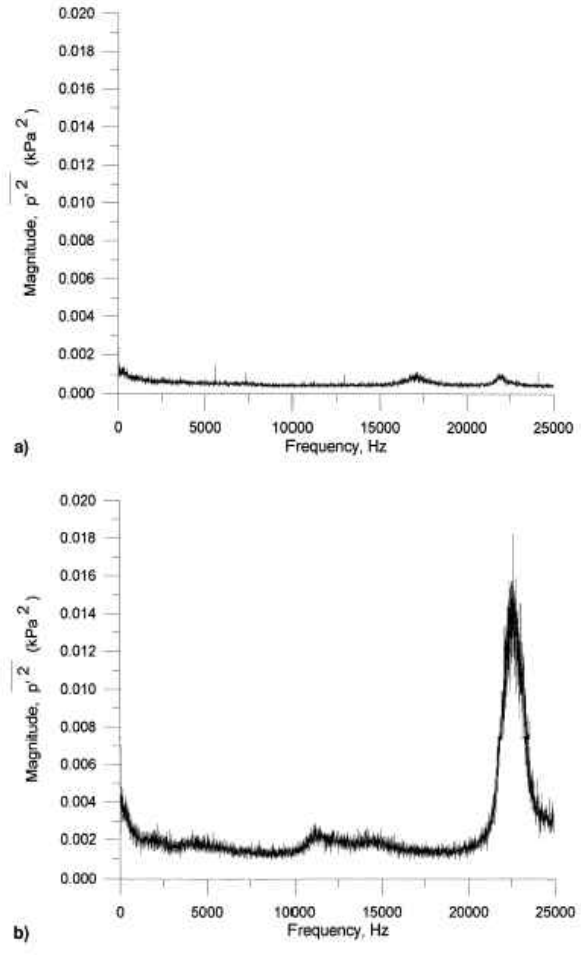

Fig. 5 Pressure spectrum a) of the upstream boundary layer and b) on the cavity floor.

boundary layer. The pressure signal produced by the upstream transducer with the cavity floor in the down position is shown in Fig. 5a. This FFT clearly shows that the signal from the upstream transducer contains a broad spectrum of low-level noise without any dominant peaks. By integrating this signal over time an SPL of 146.42 dB was determined. Likewise, examining the pressure signal obtained from the cavity transducer shows a peak pressure oscillation at approximately 23 kHz and an SPL of 161.78 dB (Fig. 5b). The amplitude of this robust peak is almost 10 times greater than the corresponding background noise within the cavity. A comparison of the SPL determined from both the upstream and cavity transducers indicates the cavity SPL is 15 dB greater than that recorded in the upstream boundary layer. Such a change in level is equivalent to the energy of the cavity oscillations increasing 32 times above that of the approaching boundary layer.

A second run was performed with the floor transducer sampled at 100 kHz to ensure that dominant frequencies above 25 kHz were insignificant. Because of the limitations of the present A/D converter, only a single channel could be simultaneously sampled at 100 kHz. Although analysis of the pressure transducer signals, using an FFT algorithm, showed a slightly higher, broader band of background noise, a single strong peak, approximately 10 times greater than the background, was still present at 23 kHz. In both cases the SPL remained constant at 161.78 and 161.76 dB, respectively.

Results and Discussion

The information presented in this section is a result of the acquisition of surface pressures within a two-dimensional open cavity. These data include time-averaged surface pressures at several locations in and around the cavity at 0-deg yaw (Fig. 6) and instantaneous pressure signals on the cavity floor. Unsteady signals were analyzed in terms of their magnitude and frequency of the dominant modes. The magnitudes of the pressure signals were integrated with respect to time and are presented as SPL at ψ = 0 (Figs. 7 and 8 for varying ψ). Figure 9 represents the spectral distribution of $\overline{p'^2}$ acquired at ψ = 45 deg. Figure 10 displays the frequencies of the first three modes as a function of ψ. These data were acquired for 25ψ between 0 and 75 deg.

Time-Averaged Surface Pressure

Figure 6 contains a comparison of the time-averaged surface pressures obtained experimentally from three separate tests at 0-deg yaw. Also included in this figure are time-averaged surface-pressure calculations performed by Tam et al.[17] When examining this plot the reader should also view Fig. 2 to identify key cavity geometry locations. In general, time-averaged cavity pressures were approximately 15% greater than the free-stream values, which is similar to the computational results reported by Rizzetta.[18] The relatively constant surface pressures observed between points *C* and *D*, i.e., streamwise along the floor, are representative of an open cavity flow.[19]

Unsteady Surface Pressures

The time-averaged properties presented in the preceding test contain no information about instantaneous events within the

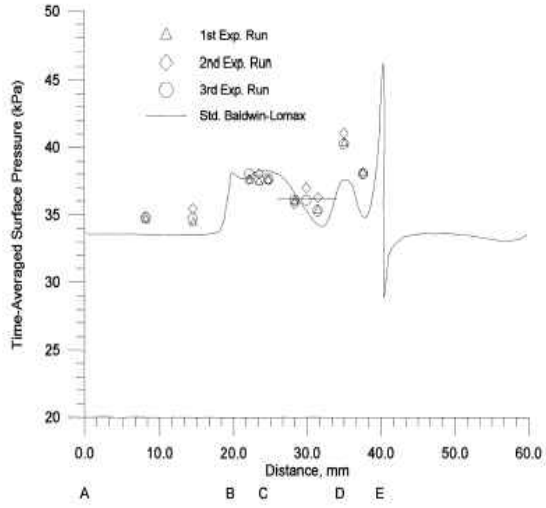

Fig. 6 Time-averaged surface pressure distribution.

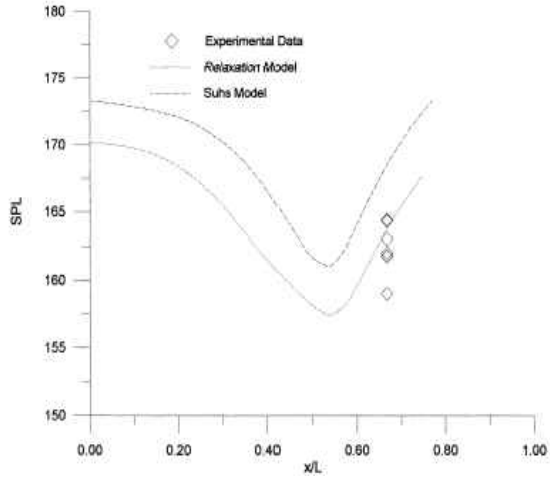

Fig. 7 Computed SPL within the cavity at ψ = 0 vs distance along the cavity floor.

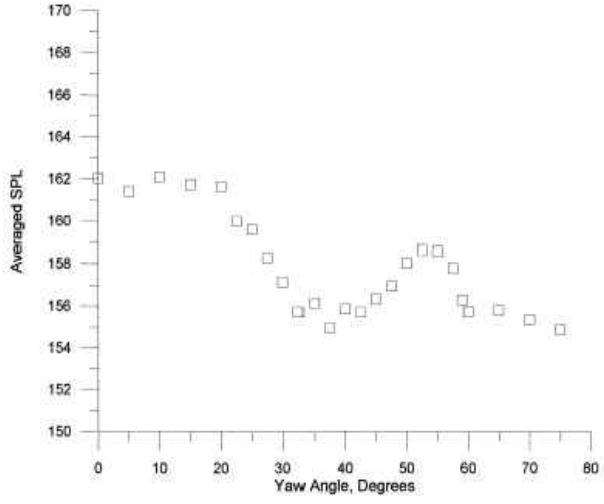

Fig. 8 $\overline{\text{SPL}}$ as a function of yaw angle.

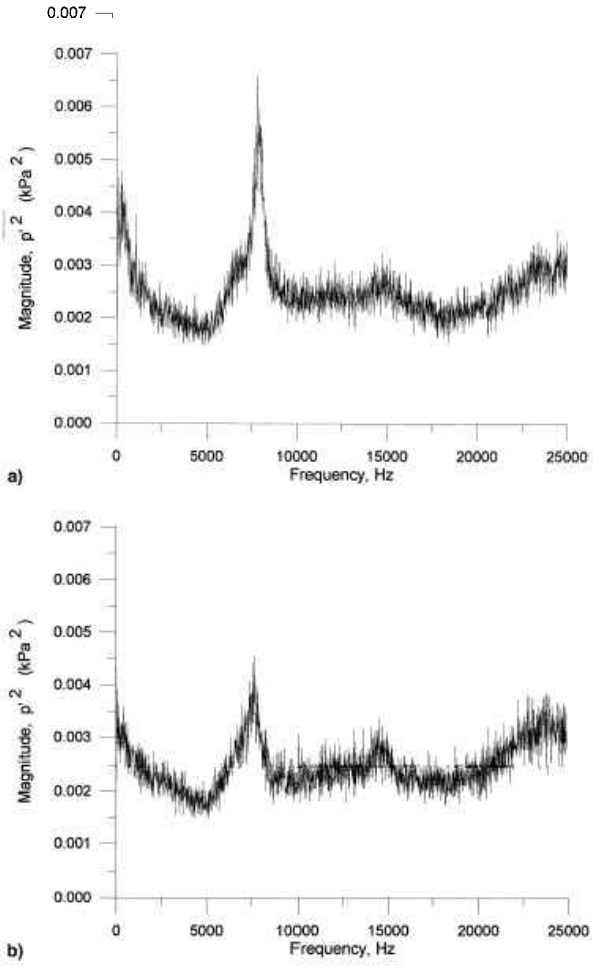

Fig. 9 FFT of the cavity pressure oscillations at 45-deg yaw a) displaying dominant mode and b) without mode dominance.

cavity. To learn more about these events, one must analyze time histories of surface properties and explore the associated frequency spectra. To that end, an FFT was used to decompose the pressure signals. The resulting FFTs display the pressure perturbation squared $\overline{p'^2}$ vs frequency (Figs. 5 and 9). Both the time-integrated magnitude and frequency content of the surface pressure signals recorded off the cavity floor transducer at different ψ are discussed next. The following sections focus

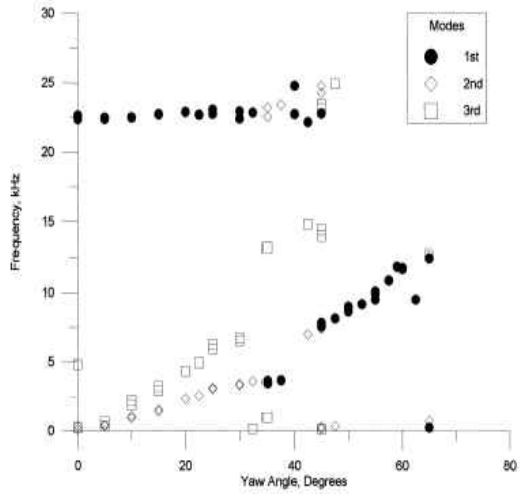

Fig. 10 Frequency of the dominant modes as a function of yaw.

on the $\overline{\text{SPL}}$ and frequency content of the transducer positioned on the cavity centerline at approximately $0.67L$.

Sound Pressure Levels

The time histories of the surface pressures were used to form time-averaged $\overline{\text{SPL}}$s within the cavity using the following equation:

$$\overline{\text{SPL}} = 10 \log_{10}(\overline{p'^2}/q_a^2) \tag{1}$$

where

$$\overline{p'^2} = \frac{1}{T}\int_{T_1}^{T_2} (p - \bar{p})^2 \, dt \tag{2}$$

The time average of the pressure fluctuations squared is normalized by q_a, 20 μPa.

Results obtained at 0 yaw are similar to those obtained by the numerical simulations presented by Tam et al. and Rizzetta. The $\overline{\text{SPL}}$ levels computed by Tam et al. at 0-deg yaw and those determined experimentally on the cavity floor at $x = 0.67L$ are shown in Fig. 7. Inspection of this figure indicates that computations using the multiple-wall approach are in good agreement with the average of the measured $\overline{\text{SPL}}$ values. This averaged $\overline{\text{SPL}}$ was determined to be 162.34 dB. With the exception of a single data point, the variation in $\overline{\text{SPL}}$ was within ± 1 dB. Further, the location of the present cavity transducer appears to correspond to a region approaching minimum $\overline{\text{SPL}}$. Based on the computed $\overline{\text{SPL}}$, variations of more than 10 dB could be expected over the length of the cavity. The average measured and computed $\overline{\text{SPL}}$ values are found to agree within 1 dB. Although such agreement may be considered excellent, it should also be noted that these plots use a decibel scale, which is logarithmic. Therefore, deceptively small differences can correspond to large pressure variations.

$\overline{\text{SPL}}$ values calculated for the cavity at yaw are presented in Fig. 8. Repeated data show that between 0 and 20 deg the $\overline{\text{SPL}}$ magnitudes appear to be relatively constant at 161.5 dB. A rapid drop in $\overline{\text{SPL}}$ was observed for $\psi > 20$ deg. Although a drop in magnitude of the dominant mode is also apparent in the FFTs, a frequency widening at the base of each peak also occurs. Similar $\overline{\text{SPL}}$ reductions were also observed by others as the flow changed from an open-cavity flow to transitional open flow and then to a transitional closed flow.[4] This drop in $\overline{\text{SPL}}$ continued and appeared to reach a minimum level of 155.5 dB, at $\psi \approx 37.5$ deg. This minimum occurs in the region where mode switching, as evident by the frequency of the dominant mode, was first observed.[20] It is important to note

that although mode switching did occur between 32.5 and 37.5 deg the amplitudes of these different dominant modes were within 50% of one another. Further, at 45 deg two different fluctuating pressure distributions were observed to exist in the cavity, as shown in Fig. 9. In most cases a dominant peak was obvious (Fig. 9a); yet in a few runs (see the FFT represented by Fig. 9b) the dominance of a single peak was weak, instead a broad spectra existed with local humps corresponding to the preferred modes. Therefore, the importance of the reported dominant mode at these ψ is questionable. Beyond 37.5 deg the averaged SPL was observed to increase, peaking at 158.5 dB. This 3-dB increase represents a doubling of the energy related to the pressure signal. Beyond 47 deg a robust dominant mode once again appears in the FFT. After 60 deg this obvious mode begins to fade into a broad region of elevated pressure. This secondary maximum was observed to occur at approximately 52.5 deg, and beyond this angle the SPL once again was observed to sharply drop off until reaching 57.5 deg. From this point forward, a linear reduction in decibels was noted until 75 deg, at which point the SPL asymptotically approached 154.5 dB.

Frequencies of the Dominant Modes

Variations in the dominant frequencies as a function of ψ are presented in Fig. 10. Inspection of this figure indicates a dominant pressure oscillation at 23 kHz. In fact, this oscillation was consistently found to exist, until a ψ of approximately 35 deg. Within this ψ range, the frequency of the dominant mode remained constant to within 500 Hz. Tracy and Plentovich[4] also reported no significant difference in the frequency content of their pressure signal. However, they only examined yaw angles of 0 and 15 deg. It is important to note that the dominant mode, i.e., the mode representing the largest amplitude, was not the first mode in the FFT. At ψ equal to 35 and 37.5 deg the dominant mode was nominally 3.55 kHz, with a secondary mode at approximately 23 kHz. This corresponded to the location where the SPL reached its minimum value (Fig. 8). However, at 40–42.5 deg the dominance of the 23-kHz mode reappears. Continuing to $\psi = 45$ deg the dominant mode is somewhat uncertain. That is, after several tests with the cavity oriented at 45 deg it was noted that, although most tests produced a dominant peak at 7.75 kHz (Fig. 9a), the dominant mode was found to switch between either 23 or 7.75 kHz. It appears that slight misalignment of the cavity yaw angle may have been responsible for this variation. Similar events were noted by Plentovich et al.[13] when very small changes in L/D caused the cavity flow to switch between transitionally opened and transitionally closed states. Although this may be true based on the criteria used to select the dominant mode, careful inspection of the associated FFT obtained at this angle clearly indicates a lack of robustness of either mode.

Existence of a second and third dominant mode was also confirmed between 0 and 37.5 deg. In either case the modes were linearly correlated with ψ up to 30 deg. Beyond $\psi = 45$ deg, the frequency of the dominant mode increased from approximately 7.75 kHz to approximately 12.5 kHz at 65-deg yaw. No secondary peaks, i.e., higher modes, were identified consistently within this range of yaw angles. Further, the slope of the third mode that was observed between 0 and 37.5 deg was approximately the same as the slope of the dominant mode observed between 45 and 65.5 deg.

A semiempirical approach used to estimate the frequency of the cavity pressure oscillations at 0-deg yaw was presented by Rossiter.[11] Rossiter's correlation related the frequency of the dominant modes within the cavity produced by vortex shedding to a modified Strouhal number. As expected, the dominant cavity frequency recorded in the present study at 0-deg yaw matched that calculated using the relationship of Rossiter

$$f_{e,m} = \frac{U_\infty}{L} \frac{(m - \gamma)}{(1/K + M)}, \qquad m = 1, 2, 3, \ldots$$

where $\gamma = 0.25$ and $K = 0.66$ are constants. This relation provided the following frequencies: $f_{e,m=1} = 9916$ Hz, $f_{e,m=2} = 23{,}138$ Hz, and $f_{e,m=3} = 36{,}360$ Hz. Rossiter also noted in his study that the dominant peak, although not necessarily the first peak, would be one of these modes. Obtaining further insight into the mechanisms that contribute to these pressure oscillations, the fundamental frequencies of the acoustic modes based on cavity L, W, and D were also approximated

$$f_L = \frac{a_T}{2L}, \qquad f_W = \frac{a_T}{2W}, \qquad f_D = \frac{a_T}{2D}$$

This results in values of f_L, f_W, and f_D equal to 11,550, 986, and 23,240 Hz, respectively.

An inspection of the frequency spectra at $\psi = 0$ deg clearly indicates a robust 22.75-kHz dominant mode with secondary peaks between 120 and 350 Hz. Because this measured fundamental mode matches f_D, it may be suggested that the dominant pressure oscillation was the result of a transverse mode, i.e., perpendicular to the cavity floor. Therefore, the transverse acoustic mode based on the cavity depth would appear to be the mechanism producing the dominant pressure oscillations observed along the cavity floor and not the mode corresponding to vortex shedding. Yet, calculations show that Rossiter's $m = 2$ mode also agrees with the present measurements to within 6%, suggesting a fluid dynamic mechanism. In addition, the $m = 2$ mode is in good agreement with computations performed by Tam et al.,[17] who found this frequency numerically, via an FFT of the pressure history at the floor centerline. Tam et al.'s computed frequency was approximately 26 kHz. In addition, recent work by the same authors[21,22] provided flowfield simulations that contained a pressure wave that reflected off the floor of the cavity. This pressure wave may represent the transverse acoustic mode.

Although a combined fluid dynamic-resonant mechanism may be the logical conclusion, the acoustic mode that produced a self-sustaining oscillation in spite of small geometric changes may indeed be the dominant driving mechanism at least until a ψ of 35 deg is attained. This result is similar to the flow transition reported by Zhang and Edwards,[23] at 0-deg yaw, in which the flow switched modes from a transverse oscillation to a longitudinal oscillation as the cavity length was increased by a factor of 3, from $L/D = 1$ and 3. However, it must be noted that accompanying this change in cavity length was a corresponding change in the planar aspect ratio W/L from 7.6 to 2.5. Therefore, it is unclear if cavity length alone was responsible for the switch from a transverse to a longitudinal mode in their study.

Mode switching in the present study, between ψ of 35 and 45 deg, was observed to produce flow oscillations of either 23 kHz or 3.5 kHz. Beyond 45 deg a permanent switch was observed. Specifically, the dominant frequency became approximately 7.7 kHz at 45 deg and increased linearly to approximately 12.5 kHz at 65-deg yaw. As previously stated, the slope of this dominant mode coincided with the slope of the third measured mode at $\psi < 35$ deg.

Recall that the longitudinal mode, which represents the fluid dynamic mechanism, is affected by many factors including the cavity geometry, M_∞, Re, and the state of the incoming boundary layer. It can be summarized that the permanent mode switch observed in the present study may be in part a result of three-dimensional edge effects, the increase in effective cavity length, and the ability of the boundary-layer flow to enter the cavity. This movement of upstream boundary-layer fluid into the cavity was made apparent using shear-stress sensitive liquid crystals placed on the cavity floor.

Summary

The effect of yaw on a two-dimensional open cavity was experimentally examined. Changes in SPL and frequency of

the dominant pressure oscillations as a function of ψ were noted. Although the $\overline{\text{SPL}}$ remained constant up to 20-deg yaw, beyond this angle the $\overline{\text{SPL}}$ dropped more than 6 dB to a minimum level at $\psi \sim 37.5$ deg. That is, the energy in the flow oscillations dropped by a factor of more than 4. This minimum corresponded to the ψ where a mode switch was observed. However, little change in dominant frequency was noted up to $\psi \sim 37.5$ deg. Comparisons of this dominant mode to the approximated fundamental acoustic frequency based on cavity depth, i.e., the transverse mode, were in excellent agreement. This suggests that the dominant mechanism for this configuration is acoustic in nature and not fluid dynamic. A variation in the secondary mode, probably fluid dynamic in nature, showed an increase in frequency as ψ was increased beyond 45 deg.

Acknowledgments

The authors thank L. Sakell and the U.S. Air Force Office of Scientific Research for their contribution through Contract F49620-93-0081. In addition, the authors greatly appreciate the engineering support of Curtis W. Fox.

References

[1]Rockwell, D., and Naudascher, E., "Self-Sustained Oscillations of Impinging Free Shear Layer," *Annual Review of Fluid Mechanics*, Vol. 11, 1979, pp. 67–94.

[2]Wilcox, F. J., Jr., "Experimental Measurements of Internal Store Separation Characteristics at Supersonic Speeds. Store Carriage, Integration and Release," Royal Aeronautical Society, London, 1990, pp. 5.1–5.16.

[3]Stallings, R. L., Jr., and Forrest, D. K., "Separation Characteristics of Internally Carried Stores at Supersonic Speeds," NASA TP-2993, March 1990.

[4]Tracy, M. B., and Plentovich, E. B., "Characterization of Cavity Flow Fields Using Pressure Data Obtained in the Langley 0.3-Meter Transonic Cryogenic Tunnel," NASA TM 4436, March 1993.

[5]Rockwell, D., and Naudascher, E., "Review: Self-Sustaining Oscillations of Flow Past Cavities," *Transactions of the American Society of Mechanical Engineers*, Vol. 100, June 1978, pp. 152–165.

[6]Issacson, L. K., and Marshall, A. G., "Nonlinear Interactions in Internal Cavity Flows," *AIAA Journal*, Vol. 21, No. 5, 1983, pp. 785, 786.

[7]Karamcheti, K., "Acoustic Radiation from Two-Dimensional Rectangular Cutouts in Aerodynamic Surfaces," NACA TN-3487, Aug. 1955.

[8]Charwat, A. F., Roos, J. N., Dewey, C. F., and Hitz, J. A., "An Investigation of Separated Flows—Part I: The Pressure Field," *Journal of Aerospace Sciences*, Vol. 28, No. 6, 1961, pp. 457–470.

[9]Charwat, A. F., Roos, J. N., Dewey, C. F., and Hitz, J. A., "An Investigation of Separated Flows—Part II: Flow Separation in the Cavity and Heat Transfer," *Journal of Aerospace Sciences*, Vol. 28, No. 7, 1961, pp. 513–527.

[10]Heller, H., and Bliss, D., "Aerodynamically Induced Pressure Oscillations in Cavities: Physical Mechanisms and Suppression Concepts," U.S. Air Force Flight Dynamics Lab., TR-75-133, Feb. 1975.

[11]Rossiter, I. E., "Wind Tunnel Experiments on the Flow Field over Rectangular Cavities at Subsonic and Transonic Speeds," Aeronautical Research Council, R&M 3438, Oct. 1966.

[12]Tracy, M. B., Plentovich, E. B., and Chu, J.,"Measurements of Fluctuating Pressure in a Rectangular Cavity in Transonic Flow at High Reynolds Numbers," NASA TM-4363, June 1992.

[13]Plentovich, E. B., Chu, J., and Tracy, M.B., "Effect of Yaw Angle and Reynolds Number on Rectangular-Box Cavities at Subsonic and Transonic Speeds," NASA TP-3099, July 1991.

[14]Baysal, O., and Yen, G.-W., "Implicit and Explicit Computations of Flows Past Cavities with and Without Yaw," AIAA Paper 90-0049, Jan. 1990.

[15]Bari, A., and Chambers, F. W., "Shear Layer Resonance over Open Cavities at Angles to the Flow Direction," AIAA Paper 93-4397, Oct. 1993.

[16]Savory, E., Toy, N., Disimile, P. J., and DiMicco, R. G., "The Drag of Three-Dimensional Cavities," *Applied Scientific Research*, Vol. 50, 1993, pp. 325–346.

[17]Tam, C. J., Orkwis, P. D., and Disimile, P. J., "A Comparison of Baldwin-Lomax Turbulence Models for 2-D Open Cavity Computations," *AIAA Journal*, Vol. 34, No. 3, 1996, pp. 629–631.

[18]Rizzetta, D. P., "Numerical Simulation of Supersonic Flow over a Three-Dimensional Cavity," *AIAA Journal*, Vol. 26, No. 7, 1988, pp. 799–807.

[19]Plentovich, E. B., Stallings, R. L., Jr., and Tracy, M. B., "Experimental Cavity Pressure Measurements at Subsonic and Transonic Speeds: Static Pressure Results," NASA TP 3358, Dec. 1993.

[20]Disimile, P. J., and Orkwis, P. D., "Effect of Yaw on Pressure Oscillation Frequency Within Rectangular Cavity at Mach 2," *AIAA Journal*, Vol. 35, No. 7, 1997, pp. 1233–1235.

[21]Tam, C. J., Orkwis, P. D., and Disimile, P. J., "Algebraic Turbulence Model Simulations of Supersonic Open Cavity Flow Physics," *AIAA Journal*, Vol. 34, No. 11, 1996, pp. 2255–2260.

[22]Tam, C. J., Orkwis, P. D., and Disimile, P. J., "Variations in Flow Field Physics Caused by Algebraic Turbulence Model Modifications for a Supersonic 2-D Open Cavity," AIAA Paper 97-0660, Jan. 1997.

[23]Zhang, X., and Edwards, J. A., "Experimental Investigation of Supersonic Flow over Two Cavities in Tandem," *AIAA Journal*, Vol. 30, No. 5, 1992, pp. 1182–1190.